Warshel, A. (1979) *Photochem. Photobiol. 30*, 285–290.
Warshel, A. (1981) *Biochemistry 20*, 3167–3177.
Warshel, A., & Ottolenghi, M. (1979) *Photochem. Photobiol. 30*, 291–293.
Warshel, A., & Russell, S. T. (1984) *Q. Rev. Biophys. 17*, 283–422.
Warshel, A., Russell, S. T., & Churg, A. K. (1984) *Proc. Natl. Acad. Sci. U.S.A. 81*, 4785–4789.

Investigation of Polylysine–Dipalmitoylphosphatidylglycerol Interactions in Model Membranes†

Danielle Carrier and Michel Pézolet*
Département de Chimie, Université Laval, Cité Universitaire, Québec, Canada G1K 7P4
Received January 2, 1986; Revised Manuscript Received March 17, 1986

ABSTRACT: The effect of poly(L-lysine) on dipalmitoylphosphatidylglycerol bilayers has been studied by Raman and infrared spectroscopies, small-angle X-ray diffraction, and carboxyfluorescein escape experiments. The polypeptide is shown to induce a stabilization of the bilayer detected by the increase of interchain vibrational coupling and a slight decrease of the overall disorder. In addition, long polylysine (M_r 150000) induces a positive shift of the gel to fluid transition temperature and, at lipid to lysine molar ratios greater than 1, a lateral phase separation within the bilayer. Raman and infrared spectra indicate modifications at the head group level. In contrast, short polylysine (M_r 4000) leads to a decrease of the lipid thermotropic transition temperature, and no modification of the polar head group and no phase separation could be observed. These differences between short and long polypeptides are correlated with the conformation the polypeptide adopts upon binding to the lipid, which favors the formation of α-helices in the case of long polylysines (M_r $\geq$14000). The X-ray data suggest that the basic polypeptide acts as a bridge between neighboring bilayers, thus causing their aggregation and dehydration.

The function of biological membranes is believed to be intimately related to their structure, which in turn strongly depends on the interactions between their main constituents, namely, lipids and proteins. In this study, we focused on a specific model system that mimics the complex formed by a peripheral protein and the lipidic surface. The binding of such proteins is primarily driven by electrostatic forces arising between their exposed positively charged residues and some negatively charged lipids of the bilayer. Owing to its strongly basic character, poly(L-lysine) (named PLL[1] hereafter) is ideally suited to model an extrinsic protein. The acidic lipid dipalmitoylphosphatidylglycerol (DPPG) was used in order to maximize the electrostatic interactions.

Polylysine has an unordered conformation at neutral pH but can form either α-helices or β-sheets in alkaline solution. In a circular dichroism study, Hammes and Schullery (1970) showed that PLL (M_r 100000) takes the α-helical conformation when it binds to natural phosphatidylserine, at neutral pH. The same effect was observed by Raman spectroscopy (Carrier & Pézolet, 1984) for dipalmitoylphosphatidylglycerol and PLL (M_r 150000). However, it was recently proposed (Carrier et al., 1985) that polylysines with lower degree of polymerization may fail to adopt such an ordered conformation upon binding to DPPG bilayers, because they did not lead to the same complex modifications of the lipid thermotropic behavior. Long poly(lysines) (M_r $\geq$60000) were shown to induce the formation of three distinct types of domains when there was less than one lysine residue per lipid molecule (R_i > 1). Our first aim was thus to verify if such lateral phase separation may be seen by Raman spectroscopy and to determine the conformation of bound polylysine of low molecular weight.

Many authors suggested that the binding of PLL to acidic lipids might also involve hydrophobic forces in addition to the straightforward electrostatic interactions. While purely electrostatic bonds are destroyed at high ionic strength, high salt concentrations (1 M NaCl) failed to completely disrupt PLL/phosphatidylserine complexes (Hammes & Schullery, 1970). From EPR spectroscopy, Hartmann and Galla (1978) concluded from the decrease of the hyperfine coupling constant of labeled polylysine that the side chains of this polypeptide penetrates into the bilayer. Shafer (1974) found that PLL exhibits a two-step mechanism of interaction with phosphatidylserine monolayers: the initial binding produces a decrease of the surface pressure, most likely due to the neutralization of lipidic head groups, followed by a gradual positive change in surface pressure that was interpreted as a consequence of the entry of the lateral side chains of the polypeptide into the lipid monolayer. This evidence that polylysine can act as a spacer between the lipidic polar heads led us (Carrier & Pézolet, 1984) to suggest the possiblity of PLL-induced interdigitation of DPPG bilayers in order to explain the change

† This work was supported by grants from National Science and Engineering Research Council of Canada and from Fonds pour la Formation de Chercheurs et Aide à la Recherche of the Ministère de l'Education of the Province of Québec. D.C. is also grateful to these organizations for postgraduate scholarships.

[1] Abbreviations: PLL, poly(L-lysine); DPPG, dipalmitoylphosphatidylglycerol; DPPC, dipalmitoylphosphatidylcholine; CF, carboxyfluorescein; LUV, large unilamellar vesicles; SUV, small unilamellar vesicles; T_c, gel to liquid-crystalline phase transition temperature; IR, infrared; E_a, activation energy.

0006-2960/86/0425-4167$01.50/0

in the packing symmetry of acyl chains observed when a molar excess of lysine residues is present. This hypothesis is questioned in this study, by use of small-angle X-ray diffraction.

Polylysine (M_r 100000) was also shown to affect the osmotic permeability of phosphatidylserine vesicles: excess polylysine made the bilayers totally permeable to sucrose (Hammes & Schullery, 1970). The authors attributed this effect to the formation of large pores within the bilayer rather than to the reorganization of closed vesicles in membrane-like sheets. We also investigated the effect of PLL on the permeability of DPPG vesicles entrapping the fluorescent dye carboxyfluorescein.

In addition to these specific questions, our ultimate goal was to shed a little more light on the molecular organization of the polylysine/DPPG complex. Infrared and Raman spectroscopies proved to be very effective in such an investigation (Chapman & Hayward, 1985; Tu, 1982) as they may give useful information about particular portions of the molecules and do not require the addition of any probe that could possibly perturb the studied system.

Materials and Methods

Materials. The ammonium salt of 1,2-dipalmitoyl-*sn*-glycero-3-phosphoglycerol (DPPG) and the bromide salts of polymyxin B, poly(L-ornithine) (M_r 25000), and poly(L-lysine) with various molecular weights were obtained from Sigma Chemical Co. and used without further purification. Carboxyfluorescein was supplied by Eastmann-Kodak and purified according to the method of Weinstein et al. (1981).

Raman Measurements. A 1–4% by weight stock lipidic dispersion was prepared by adding 100 mM phosphate buffer, pH 7.0, to the weighed lipid and submitting this mixture to three or four cycles of heating (55 °C)–vortex shaking–cooling (15 °C). The required amounts of polypeptide solutions were then added to aliquots of this dispersion, and each sample was subjected to the thermal treatment mentioned above before being transferred into a glass capillary. This latter was centrifuged to yield a white pellet used for the measurements. In a previous study (Carrier & Pézolet, 1984), it was shown that essentially all polylysine is bound at $R_i \geq 1$ while part of it remains in the supernatant at lower R_i.

Samples were irradiated with 514.5-nm line of an argon ion laser (Model 165, Spectra-Physics Inc.) at ~200 mW power at the sample. Spectra were recorded with a computerized spectrometer (Model 1400, Spex Industries Inc.) described elsewhere (Savoie et al., 1979), with a spectral resolution of 5 cm^{-1}. The monochromator was calibrated with a neon discharge lamp, and the frequencies cited later are believed to be accurate to ±2 cm^{-1} for sharp peaks.

Spectra were computer-corrected for the solvent contribution by subtracting its spectrum multiplied by an appropriate factor, chosen as to obtain a straight base line between 1720 and 1900 cm^{-1} in the corrected spectra. If needed, spectra were then corrected for fluorescence backgrounds by substracting appropriate polynomial functions (Savoie et al., 1979).

Infrared Measurements. The weighed dry lipid was hydrated with the polypeptide solution and submitted to the same thermal treatment as Raman samples. The mixture was then transferred between two heated (~55 °C) CaF_2 windows with a 7-μm Mylar spacer and allowed to form a uniform film at this temperature before the beginning of the experiment.

Spectra were recorded with a Bomem DA3-02 Fourier-transform infrared spectrophotometer with a mercury–cadmium–telluride detector and a KBr beam splitter. A total of 1000 scans was routinely taken, with a maximal optical retardation of 0.5 cm, and they were triangularly apodized, zero-filled once, and Fourier transformed to yield a resolution of 2 cm^{-1}.

Small-Angle X-ray Measurements. Appropriate volumes of the DPPG dispersion and the polypeptide solution were introduced with a syringe into an X-ray thin-walled glass capillary to give the desired R_i value. Capillaries were sealed and centrifuged many times to ensure proper mixture.

X-ray diffraction experiments were performed with a Warhus-Statton camera, using nickel filtered Cu Kα line (λ = 0.154 nm) at an anode loading of 40 kV and 25 mA. The photographic plates were placed at 32 cm from the sample, in an evacuated enclosure. Exposure times were typically of 1–3 days, but diluted lipidic dispersions required much longer exposures.

Carboxyfluorescein Fluorescence Measurements. Large unilamellar vesicles (LUV) were prepared by the reversed-phase evaporation technique of Szoka and Papahadjopoulos (1978), in order to get vesicles with a diameter of the order of 460 nm (Wilschut, 1982). A total of 25 mg of DPPG was dissolved in 2 mL of benzene–methanol (200:7), and a small volume of a solution of phosphatidylcholine labeled with ^{14}C was added to allow the determination of DPPG concentration in the final LUV preparation. The mixture was lyophilized and redissolved in 1.8 mL of diethyl ether–methanol–chloroform (15:2:1) by heating over hot water to obtain a clear solution. A total of 500 μL of carboxyfluorescein 200 mM in 20 mM phosphate buffer and 1 mM EDTA, pH 7.5, was added to this solution which was sonicated a few minutes on a bath-type sonifier, at temperatures increasing from 0 to 35 °C during sonication. The clear sonicate was then evaporated (rotary evaporator, 200 rpm) for 1 h at 25 °C until it formed a gel. A total of 1 mL of buffer was added, and the mixture was evaporated again, at 45–50 °C, and let at ~18 °C overnight. The preparation was eluted on Sephadex G-50 with the same buffer as eluent, and LUV were collected in the head fractions. Aliquots of the latter were analyzed for their radioactive contents, and DPPG concentrations were calculated.

The CF fluorescence measurements were performed on a SLM 8000 spectrofluorometer, with an excitation wavelength of 490 nm and an emission wavelength of 515 nm. Temperature was regulated by circulation of thermostated water. Polylysine solution was added with a syringe directly into the cell and quickly mixed.

Results

Raman and IR Measurements. The Raman bands due to C–H stretching vibrations are very sensitive to the molecular order within the bilayer. Figure 1 shows that increasing temperature results in a lowering of the intensity ratio h_{2880}/h_{2845} of the bands at 2880 and 2845 cm^{-1} assigned respectively to the antisymmetric and symmetric vibrations of the acyl chain methylenes. This effect has been related to the reduction of the interchain Fermi interactions producing an underlying broad band around 2880 cm^{-1} (Gaber & Peticolas, 1977) and to the increase of the acyl chain rotational mobility (Snyder et al., 1980). Therefore, this intensity ratio may be used to monitor the intermolecular vibrational coupling of the acyl chains.

The second intensity ratio shown in Figure 1, h_{2930}/h_{2880}, is used as a measure of the overall disorder of the lipid acyl chains matrix (Dasseux et al., 1984; Bunow & Levin, 1977). Its increase at high temperature results from an apparent increase of the methyl symmetric stretching at 2930 cm^{-1}, which has been attributed to the appearance of an underlying infrared-active methylene asymmetric stretching mode becoming Raman allowed as the low-temperature chain sym-

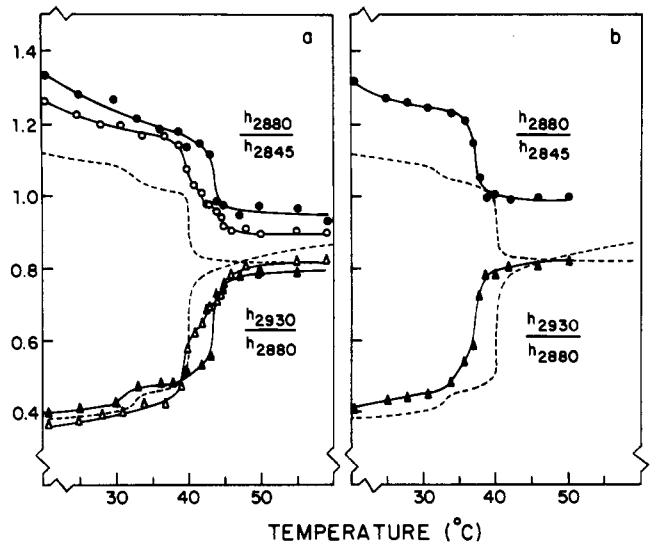

FIGURE 1: Temperature profiles for a pure DPPG dispersion (dotted lines) and DPPG/PLL complexes at $R_i = 5$ (open symbols) and $R_i = 1$ (solid symbols) for polylysine with M_r (a) 150000 and (b) 4000.

metry is destroyed (Bunow & Levin, 1977).

On the pure lipid temperature profiles (Figure 1, dashed lines), both ratios indicate a sharp transition at 40 °C corresponding to the gel to liquid-crystalline phase transition and a small pretransition at ~33 °C. With long polylysine (M_r 150000) at $R_i = 1$, the main transition is shifted to 45 °C (Figure 1a). According to the intensity ratio h_{2880}/h_{2845}, this polylysine induces an important increase of the interchain interactions on the whole range of temperature. At $R_i = 5$, the triphasic transition observed on the temperature profile indicates the formation of three distinct phases, one melting at the same temperature as the pure lipid, another with the same transition temperature as the equimolar complex, and, finally, a third one with an intermediate transition temperature (42 °C). With a short polylysine (M_r 4000), the effects are completely different. At $R_i = 1$, the temperature profiles (Figure 1b) show a decrease of 3 °C of the lipid transition temperature instead of a 5 °C increase. However, there is also a strong augmentation of interchain interactions (as seen by the h_{2880}/h_{2845} ratio).

The curves presented in Figure 1 are not corrected for the buffer and polypeptide spectral contributions. It has been shown previously (Carrier & Pézolet, 1984) that these corrections do not change significantly the intensity ratio found for dispersions of the pure lipid while for an equimolar DPPG/PLL complex the h_{2930}/h_{2880} ratio is reduced by approximately 0.05 because of the contribution of the band associated with the C–H stretching vibration of polylysine at 2920 cm^{-1}. Therefore, PLL induces a small decrease of the intermolecular disorder within the bilayer.

In view of the difference in the effects of short and long PLL on the thermotropic behavior of DPPG, it was interesting to compare the structure adopted by these PLL when bound to DPPG bilayers at neutral pH. Figure 2 shows the Raman spectrum of various DPPG/PLL complexes in the amide I region (1630–1680 cm^{-1}). The equimolar DPPG/PLL complex with long polylysine (M_r 150000) gives rise to an amide I band that almost perfectly coincides with that of α-helical PLL, thus showing that bound polylysine has formed α-helices. At $R_i < 1$, the high-frequency shoulder on the amide I band (spectrum 2b) indicates the prescence of unordered bound PLL in addition to the helical polypeptide. On the other hand, short polylysine (M_r 4,000) remains in the random-coil conformation

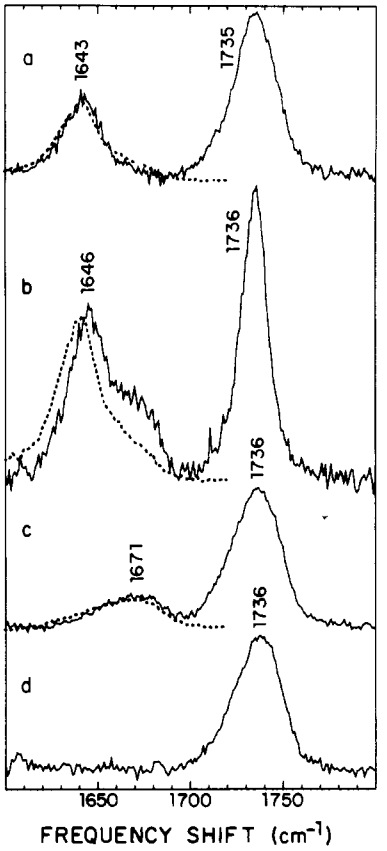

FIGURE 2: Raman spectra of the amide I and carbonyl region for (d) pure DPPG dispersion and DPPG/PLL complexes with polylysine with M_r 150000 at a lipid to lysine molar ratio of (a) 1 and (b) 0.3 or (c) with polylysine with M_r 4000 at an equimolar lipid to lysine ratio. Spectra were taken at 20 °C and are corrected for the water spectral contribution. Dotted lines are for aqueous solutions of PLL in (a and b) the α-helical and (c) random-coil conformations.

in the equimolar DPPG–lysine residue complex (spectrum 2c).

The straightforward question then is to know if short polylysine can in fact form α-helices in the conditions where long polylysine do. The samples used to obtain spectra a, c, and e in Figure 3 were prepared under identical conditions, except for tiny variations in pH. Polylysine with M_r 25000 gives a spectrum (Figure 3c) with the same characteristics of the α-helical conformation as long PLL with M_r 150000: (1) the amide I peak is sharp and appears at 1641 cm^{-1}, and (2) there is no apparent amide III band around 1250 cm^{-1}. Spectrum 3a shows that at high pH the conformation of PLL with M_r 4000 is only partly converted to the α-helical one since there is only a small decrease of the intensity of the amide III peak and a minor shift of the amide I band to lower frequency. In order to get a deeper understanding of the DPPG–PLL interaction, we also undertook some experiments with poly(L-ornithine) (M_r 25000), a homologue of polylysine with shorter side chains. As short polylysine, poly(L-ornithine) exhibits an incomplete conformational transformation at high pH (Figure 3e). However, DPPG proved to be effective to induce the formation of α-helices by this polypeptide (Figure 3g).

Besides the difference of effects of short and long PLL on the thermotropic behavior of DPPG, they also exhibit unlike influences on the lipid head group. In Figure 2, one can see the reduction of half-width of the lipid carbonyl stretching band induced by long polylysine (spectrum a) compared to the situation with short polylysine (spectrum c) and for the pure lipid (spectrum d). The half-width decrease is dramatically enhanced when long PLL is in excess. The same effect is also observed in the infrared spectra (Figure 4), where

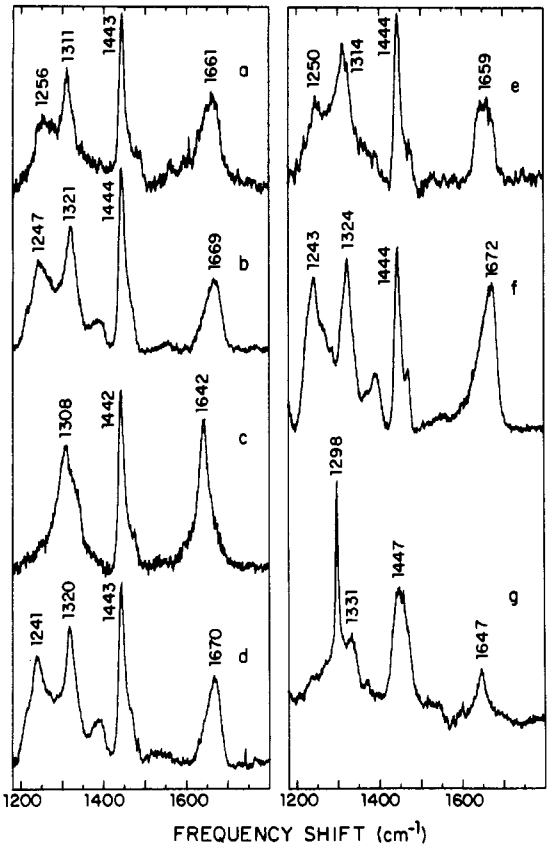

FIGURE 3: Raman spectra of polylysine with M_r (a and b) 4000 and (c and d) 25 000 and (e and f) of poly(L-ornithine) with M_r 25 000. Spectra a, c, and e were taken at 4 °C, pH ~11.9, and polypeptidic concentration of ~1.7% by weight. Spectra b, d, and f were taken at 20 °C, neutral pH, and polypeptidic concentration of ~3% by weight. All spectra are corrected for the water spectral contribution. (g) Raman spectrum of DPPG-bound poly(L-ornithine) with M_r 25 000 at 20 °C, after subtraction of the pure lipid dispersion and buffer (100 mM phosphate, pH 7.0) spectral contributions.

Table I: Characteristics of DPPG Carbonyl Band

complex	R_i[a]	Raman spectrum frequency (cm⁻¹)	Raman spectrum half-width (cm⁻¹)	IR spectrum frequency (cm⁻¹)	IR spectrum half-width (cm⁻¹)
DPPG		1736	31	1738	33
DPPG/PLL	1	1736	31	1738	34
(M_r 4000)	0.1			1739	33
DPPG/PLL	1	1735	28	1738	30
(M_r 150 000)	0.1			1738	30
	0.03	1736	16		

[a] Number of lipid molecules per lysine residue at preparation.

short polylysine shows no effect on the carbonyl band half-width at 20 °C while long polylysine produces a marked narrowing of this spectral feature. These changes are summarized in Table I.

At this point, we feel that the importance of the thermal history of the sample should be stressed. It has been reported (Carrier & Pézolet, 1984) that a slow modification of the acyl chains packing symmetry occurs for DPPG/PLL (M_r 150 000) at $R_i \leq 1$. This change was monitored by the splitting of the methylene deformation mode and was reversed by simple heating above the pretransition temperature. As seen on Figure 5, polylysine with M_r 40 000 leads to the same process: the peak at 1420 cm^{-1} in the first spectrum at 20 °C (spectra were taken from the bottom to the top) disappears after heating the sample at 36 °C. This change can be paralleled with other modifications of the Raman spectrum. The carbonyl band of DPPG is sharper and appears at a slightly lower

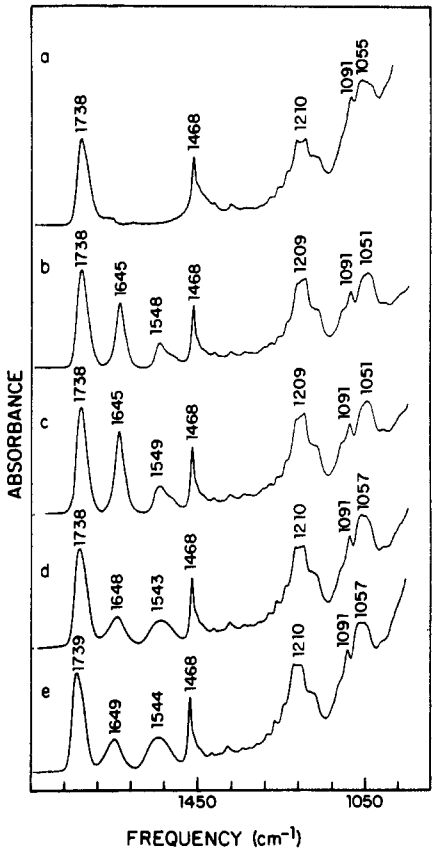

FIGURE 4: Infrared spectra of (a) pure DPPG dispersion and of DPPG/PLL complexes with polylysine having M_r 150 000 at lipid to lysine molar ratio of (b) 1 and (c) 0.1 or M_r 4000 at lipid to lysine molar ratio of (d) 1 and (e) 0.05. All spectra were taken at 20 °C and are corrected for the buffer (100 mM phosphate, pH 7.0) spectral contribution.

Table II: Lamellar Repeat Distances of DPPG Complexes

complex	R_i[a]	age of sample (days)	lamellar repeat distance (nm, ±0.05)
DPPG (90% w/w in water)		1	5.85
DPPG/PLL	0.1	9	5.87
(M_r 150 000)	0.1	29	5.90
	1	2	6.12
	5	1	6.08
DPPG/PLL (M_r 4000)	1	5	5.41
DPPG/poly(L-ornithine) (M_r 25 000)	0.1	20	5.51
	1	1	5.56
DPPG/polymyxin B	5	30	4.49
	10	3	4.44
DPPG/Ca^{2+}	1	1	5.18

[a] Number of lipid molecules per lysine or ornithine residue or per polymyxin molecule or calcium ion at preparation.

frequency when the acyl chains adopt this new chain-packing lattice, the intensity ratio h_{2880}/h_{2845} is larger, and the overall profile of the congested 700–1000-cm^{-1} region is modified.

The infrared spectrum (Figure 4) also reveals a shift of the band attributed to the P–O vibration of the phosphodiester group from 1055 (Arrondo et al., 1984) to 1051 cm^{-1} in the presence of PLL with M_r 150 000 at $R_i \leq 1$. The bands due to symmetric (1091 cm^{-1}) and antisymmetric (1220 cm^{-1}) PO_2^- stretching vibrations were not modified. Short polylysine (M_r 4000) failed to produce any significant change of the phosphate group vibrations.

Small-Angle X-ray Diffraction. The X-ray measurements reveal a lamellar repeat distance of 6.12 nm for the equimolar

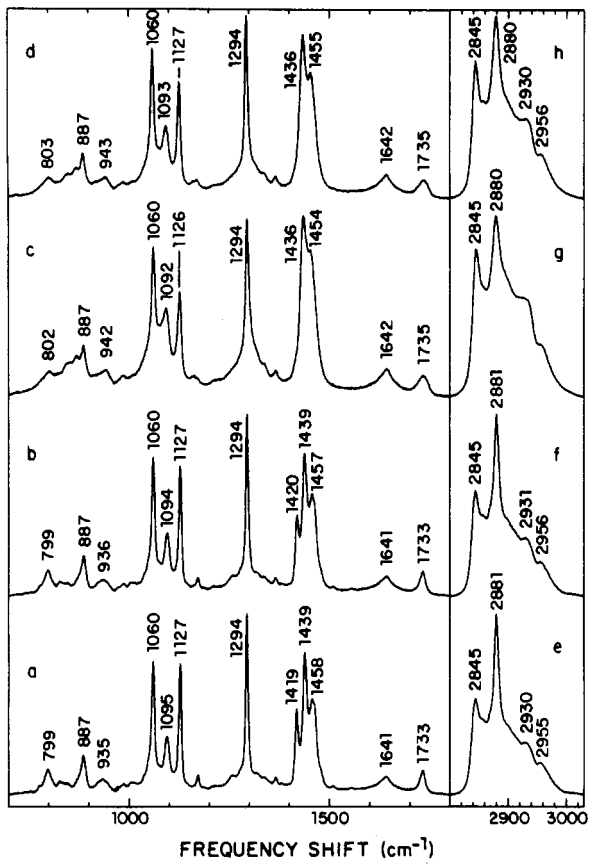

FIGURE 5: Raman spectra of a DPPG/PLL (M_r 40 000) complex at a lipid to lysine molar ratio of 0.3, after 38 days at 5 °C. The spectra were taken in the following order: (a and e) at 4 °C; (b and f) at 20 °C; (c and g) at 36 °C; (d and h) at 20 °C.

DPPG/PLL (M_r 150 000) complex (Table II). At $R_i = 5$, where the lateral phase separation is expected to occur, we have only found reflections indicating a single 6.08-nm repeat distance. In the presence of excess polylysine, X-ray measurements indicate a slightly smaller lamellar repeat distance of 5.87 nm, which do not change significantly with time. The equimolar DPPG/PLL (M_r 4000) complex exhibits a lamellar distance of 5.41 nm. For complexes with poly(L-ornithine) (M_r 25 000), the X-ray measurements indicate repeat distances of 5.56 and 5.51 for $R_i = 1$ and $R_i = 0.1$, respectively.

Experiments with Carboxyfluorescein. The curve of the intensity of diffused light (360 nm) at increasing temperature for a diluted aliquot of large unilamellar vesicles (LUV) containing carboxyfluorescein (CF) shows that the lipid undergoes a gel to fluid transition at 39.2 °C, which coincides fairly well with the transition temperature of multilamellar DPPG liposomes, ~40 °C.

Figure 6 shows the variation of CF fluorescence induced by the addition of specific amount of PLL (M_r 4000). The fluorescence of CF molecules is quenched inside the vesicles because of nonradiative deactivation processes occurring at high dye concentration. Upon dilution, the fluorescence of CF is restored. Complete fluorescence recovery (100 on the Y axis) is obtained by total lysis of the encapsulating vesicles with Triton X-100. Therefore, it is evident from Figure 6 that short PLL has a rather minor effect, which is maximal around $R_i = 2$. Lower polypeptide concentration ($2 < R_i \leq 200$), as well as higher concentration ($1 > R_i > 0.01$), gave smaller effects. Long polylysine (M_r 180 000) proved to be less effective than short PLL.

Figure 7 shows the Arrhenius plot obtained with PLL (M_r 4000) at $R_i = 7$, over the 15–35 °C temperature range. It

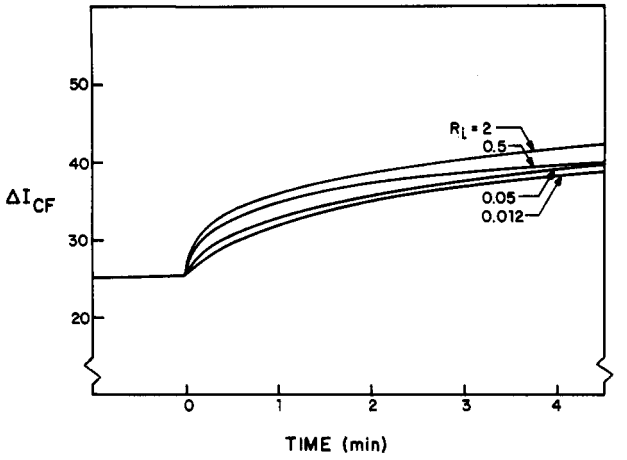

FIGURE 6: Variation of fluorescence of carboxyfluorescein entrapped in DPPG large unilamellar vesicles upon addition of PLL (M_r 4000) at various lipid to lysine molar ratios (R_i). Maximal fluorescence intensity (100 on Y axis) was determined by subsequent addition of Triton X-100.

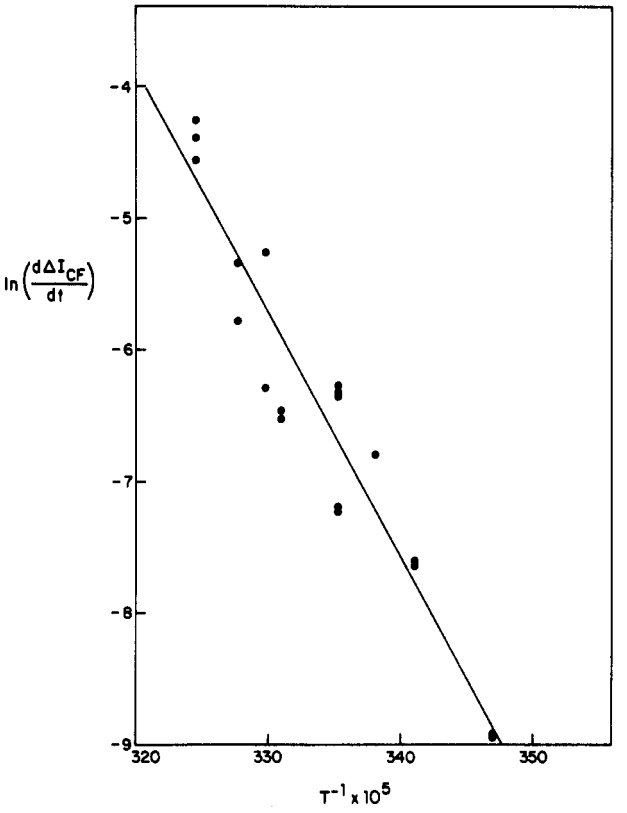

FIGURE 7: Arrhenius plot of variation of fluorescence of carboxyfluorescein entrapped in DPPG large unilamellar vesicles upon addition of PLL (M_r 4000) to give a lipid to lysine molar ratio of 7, over a temperature range of 15–35 °C.

gives an activation energy of 155 kJ·mol^{-1} while a similar plot in the absence of PLL led to a value of 100 kJ·mol^{-1}. Before the final lysis with Triton X-100, each sample used to derive Figure 7 was submitted to a hypertonic shock resulting from the addition of concentrated NaCl to get a final salt concentration of 150 mM. Under the effect of this osmotic unbalance, the vesicles shrink through expulsion of water. For this process, an activation energy of 95 kJ·mol^{-1} was found.

Discussion and Conclusions

This study confirms our previous finding (Carrier et al., 1985) that the degree of polymerization of polylysine is a key parameter to understanding the interactions of DPPG with

this polypeptide. Phase separations induced by PLL have previously been reported (Galla & Sackmann, 1975a,b; Hartmann et al., 1977; Hartmann & Galla, 1978), but it now appears that such phenomena may not be produced by all lysine homopolymers.

Despite the important difference in lipidic concentration between the two techniques, the phase transition temperatures found by Raman spectroscopy for DPPG/PLL (M_r 150000) at R_i = 5 coincide within 1 °C with those obtained from diphenylhexatriene fluorescence polarization measurements (Carrier et al., 1985). The lowest melting temperature probably corresponds to domains of unperturbed lipids, which may reasonably be expected at R_i = 5. The highest transition temperature, 45 °C, approximately falls in with that found at equimolar DPPG/lysine ratio for PLL with M_r 150000. It most likely results from patches of lipids bound according to a 1:1 stoichiometry. Finally, it has been proposed that the intermediate transition pertains to domains having a different overall stoichiometry, possibly through asymmetric binding of polylysine on only one side of the bilayer.

The increase of h_{2880}/h_{2845} intensity ratio in the Raman spectrum of DPPG caused by long as well as by short PLL, in both liquid-crystalline and gel phases, indicates an enhancement of the interchain interactions (Figure 1). This increase of interactions between acyl chains could be attributed, at least partly, to the tightening of the head group lattice resulting from charge neutralization. However, the experiments of Shafer (1974) have indicated that a larger expansion of the monolayer on addition of polylysine follows this initial compression. According to Watts et al. (1981), DPPG acyl chains are tilted with an angle of 30° relative to the bilayer normal when the head groups are in the charged state, and charge neutralization through change of pH results in the reduction of the tilt angle to less than 5°. A pH-induced increase of interchain interactions in DPPG bilayers has also been observed by Raman spectroscopy (M. Lafleur, R. Kouaouci, and M. Pézolet, unpublished results). The straightening of acyl chains leads to an increase of interchain interactions because of longer section of each chain may interact with its neighbors. Therefore, we believe that the decrease of tilt angle is the major explanation for the higher h_{2880}/h_{2845} intensity ratio for DPPG/PLL complexes at $R_i \geq 1$. At lower molar ratios, the additional effect is attributed to the modification of the packing symmetry of the acyl chains from hexagonal to orthorhombic unit cells (Synder et al., 1978, 1980). According to the intensity ratio h_{2930}/h_{2880}, long PLL also induces a small increase of the molecular order in the bilayer.

Besides the similar increase of interchain interactions and overall order, the effect of polylysine with M_r 4000 on DPPG is quite different. No lipidic phase separation is observed, and the gel to liquid–crystalline transition is shifted by 3 °C to lower temperatures. In addition, the transition temperature for the equimolar complex was less reproducible than with other PLL: over ten samples, two had a T_c differing by 3 °C or more from the average. Diphenylhexatriene fluorescence polarization (Carrier et al., 1985) has indicated no significant change—or very small increase—of the lipid transition temperature and no phase separation over a wide range of molar ratios. This difference between the results of the two techniques and the lack of reproducibility in Raman experiments suggest that kinetic factors might be involved. It seems that in this case the aggregation happens so suddenly that the polar heads do not always have enough time to adjust in the best way at the interface. Under the conditions of diphenylhexatriene experiments, the process is slowed down because the DPPG concentration is much lower. But, what could be the primary reason for this discrepancy between long and short PLL, and why does one lead to lateral phase separation and not the other?

The Raman results presented here now provide an unambiguous answer: these differences correlate with the structure adopted by the polypeptide upon binding. Long PLL with M_r 150000 (Carrier & Pézolet, 1984) or 100000 (Hammes & Schullery, 1970) are known to be in the α-helical conformation when bound to acidic lipids. This mass range can be extended down to 14000 (unshown Raman results). In the fluorescence study cited above, all these PLL led to phase separation at proper R_i, although the phenomenon was different for the so-called medium (M_r 14000–17000) and long PLL (M_r ≥60000). On the other hand, no phase separation occurs with short polylysine, which remains in the random-coil conformation after binding. In this case, the lipid still experiences the effects of an electrostatic binding, but the interaction is not influenced by the constraint of a given regular spacing between lateral amino groups.

In principle, a chain containing 15–20 amino acids should be able to form an α-helix. The Raman spectra in Figure 3 show that shorter chains less readily form helices in the same conditions. The potentiality for helix formation also depends on the nature of the amino side group, and ornithine is known to be less helix stabilizing than lysine (Chaudhuri & Yang, 1968). This is confirmed in Figure 3, where polylysine with M_r 25000 exhibits the spectral characteristics of almost purely α-helical conformation while poly(L-ornithine) with the same molecular weight seems to be halfway between α-helix and random coil. However, DPPG appears to be efficient in inducing the formation of α-helices by this polypeptide (Figure 3g). A poor tendancy to form α-helices thus seems to be overcome by the lipid when the polypeptide degree of polymerization is high enough.

Raman and infrared spectra (Figures 2 and 4) also demonstrate differences between the effects of short and long PLL at the head group level of the lipid. In the presence of long PLL at R_i = 1, the half-width of the bands associated with the acyl carbonyl stretching vibration, at 1736 (Raman) or 1738 cm^{-1} (IR), slightly decreases (Table I). The narrowing is more pronounced with an excess of long polylysine. The physical significance of this narrowing of the carbonyl band is not straightforward since it has been shown that for most lipids this spectral feature can be resolved into two components (Casal & Mantsch, 1984; Dluhy et al., 1983). After resolution enhancement by the Fourier deconvolution proceedure (Kauppinen et al., 1981), we have observed that the 1738 cm^{-1} feature in the infrared spectrum of DPPG is composed of a strong band at 1740 cm^{-1} and a weak unresolved shoulder at approximately 1725 cm^{-1}. These two components have been assigned (Bicknell-Brown et al., 1980; Levin et al., 1982) to C=O stretching vibrations of carbonyl groups with trans and gauche conformation about the C_2–C_1 bond in the ester linkage, respectively. Since the 1725-cm^{-1} band is very weak in the deconvolved spectrum of DPPG, the two carbonyl groups appear to be more equivalent than in the case of DPPC (Casal & Mantsch, 1984). The narrowing of the deconvolved 1738-cm^{-1} band (Table I) on addition of long polylysine results from the partial disappearance of the 1725-cm^{-1} shoulder. Therefore, in the presence of long PPL, the C=O groups of DPPG are even more equivalent than those for the pure lipid. Addition of short polylysine to DPPG does not affect the intensity of the 1725-cm^{-1} shoulder. In addition, the signal

associated with the P–O stretching of the phosphate diester group in the infrared spectra is shifted to lower frequencies, possibly because of hydrogen-bond formation (Arrondo et al., 1984). The absence of these modifications when short PLL is substituted to the long one confirms that their mode of action is different at the level of DPPG polar head. In a ^{31}P NMR study, Smith et al. (1983) concluded that the binding of short PLL with phosphatidylserine does not imply long-lived associations between individual lysyl groups and lipidic head groups but that each lysyl residues experiences a global attractive field at the bilayer.

In a previous study, the passage of the DPPG acyl chains packing from hexagonal to orthorhombic symmetry in the presence of excess long PLL was associated with the possible interdigitation of the lipid chains (Carrier & Pézolet, 1984). However, in the light of our X-ray results (Table II), this latter hypothesis may be eliminated. DPPG/polymyxin (5:1) is known to give interdigitated bilayers (Theretz et al., 1983), and we have measured a lamellar repeat distance of 4.5 nm in this case, the same value as reported by Ranck and Tocanne (1982). In contrast, complexes with long polylysine lead to values of the order of 6.1 nm at $R_i \geq 1$, where the acyl chains are still packed in a hexagonal array. At lower molar ratio, the lamellar repeat distance is only slightly reduced (5.9 nm), even after 1 month at low temperature to ensure a maximal conversion to orthorhombic subcell. This mere 0.2-nm variation with excess PLL clearly discredits the interdigitation hypothesis.

The experiments with large unilamellar vesicles entrapping carboxyfluorescein shed some light on the interaction of short polylysine with DPPG bilayers. First, this polypeptide does not induce the abrupt lysis previously seen upon addition of PLL (M_r 30000–70000) to cardiolipin small unilamellar vesicles (Gad et al., 1982) but gives only smooth effects at any molar ratio. While the process of spontaneous CF escape in the absence of PLL—that is, the spontaneous burst of LUV—has an activation energy E_a of 100 kJ·mol^{-1}, we observe a value of 155 kJ·mol^{-1} when short PLL is added to give a R_i = 7. The simple lysis by polylysine would rather give a decreased activation energy. PLL addition indeed causes some CF dilution, but the identification of this process is not straightforward. Hampered lysis is consistent with the increase of E_a, but it cannot justify the decrease of the polypeptide effect at high concentration. The coincidence of maximal effect with the binding stoichiometry (this was checked with two different lots of LUV) suggests a possible relation with the DPPG/PLL complex formation. Kimelberg and Papahadjopoulos (1971) have proposed that the asymmetric charge distribution produced when PLL binds to one side of the bilayer could promote the flip-flop of this patch. Partial loss of internal content could occur during this inversion. At low polylysine concentration, the CF escape would be reduced because of the lower number of PLL-bound patches per vesicle. At high PLL concentration, CF escape could well be impeded by the presence of dangling ends of noncompletely bound polypeptidic chains. A second explanation can also be put forward. According to Shafer (1974), polylysine induces a lateral expansion of the bilayer. The expansion of the membrane allows the vesicles to swell and the entry of water implies a certain CF dilution. However, the water permeability of the bilayer is gradually decreased at lower R_i, and the swelling is consequently reduced. This permeability reduction is confirmed by the diminution of LUV reaction to hypertonic shock when PLL is present (unshown results). A third possibility is the spillage of internal content that could occur during PLL-induced fusion of LUV. Polylysine (M_r 30000–70000) is known to promote the fusion of acidic liposomes (Gad, 1983) and small unilamellar vesicles (Gad et al., 1982).

In conclusion, what can we say about the molecular organization of the PLL/DPPG complexes? Polylysines with $M_r \geq 14000$ form an α-helix when they bind to DPPG bilayers, at neutral pH. A number of evidences favor a 1:1 stoichiometry between the amino side chains and the lipidic molecules. The binding of all PLL lateral groups to the same bilayer could be feasible if a certain penetration of inner lysyl groups into the lipidic head groups was allowed. But such a model is very unlikely for poly(L-ornithine), which behaves similarly to PLL in our study. According to Harmann and Galla (1978), only half of lysines are bound. If this were so, each lipidic surface would be covered with one layer of polypeptide and the outer unbound amino groups should be charged and hydrated. Consequently, distinct bilayers would repel each other because of their positively charged character. This scheme is totally inconsistent with our X-ray results. If one considers that a DPPG bilayer has approximately a total thickness of 4.8 nm and that the core of an α-helix roughly measures 0.4 nm to which one must add the space occupied by the side chains, the possibility of having two layers of polylysine plus a layer of insulating water is clearly excluded because the lamellar repeat distance would largely exceed the 6.1 nm found at $R_i \geq 1$. Actually, this X-ray result indicates that the space between neighboring bilayers is not large enough for more than a single α-helix, with the amino lateral chains pointing toward the nearest lipidic surface. This "bridge model" justifies the dehydration caused by PLL and explains why it destroys unilamellar vesicles, forming stacked bilayers. It is also nicely confirmed by the slightly smaller lamellar repeat distance found with poly(L-ornithine), 5.6 nm. Such a bridge model has been proposed for calcium-bound DMPA and DPPA by Liao and Prestegard (1981).

With short polylysine, there is no ordering of the polypeptide in α-helix form, no change of the acyl chains packing symmetry at any molar ratio, and no apparent modification of DPPG head group. However, there is still a marked increase of interchain interaction and a reduction of overall disorder in the bilayer. The lamellar repeat distance (5.4 nm) is consistent with the hypothesis that the unordered short PLL also forms bridges between DPPG bilayers. In addition, this model justifies the strong aggregating and dehydrating power of short polylysine and might be a clue to the understanding of fusion processes.

ACKNOWLEDGMENTS

We are indebted to G. Laroche for performing the X-ray diffraction measurements and to J. Dufourcq from the Centre de Recherches Paul Pascal, France, for several thoughtful discussions and for his invaluable assistance regarding the carboxyfluorescein escape experiments.

Registry No. PLL, 25104-18-1; DPPG, 4537-77-3; Ca, 7440-70-2; poly(L-ornithine), 25104-12-5; polymyxin, 1404-26-8.

REFERENCES

Arrondo, J. L. R., Goni, F. M., & Macarulla, J. M. (1984) *Biochim. Biophys. Acta 794*, 165–168.

Bicknell-Brown, E., Brown, K. G., & Person, W. B. (1980) *J. Am. Chem. Soc. 102*, 5486–5491.

Bunow, M. R., & Levin, I. W. (1977) *Biochim. Biophys. Acta 487*, 388–394.

Bush, S. F., Levin, H., & Levin, I. W. (1980) *Chem. Phys. Lipids 27*, 101–111.

Carrier, D., & Pézolet, M. (1984) *Biophys. J. 46*, 497–506.

Carrier, D., Dufourcq, J., Faucon, J.-F., & Pézolet, M. (1985) *Biochim. Biophys. Acta 820*, 131–139.
Casal, H., & Mantsch, H. H. (1984) *Biochim. Biophys. Acta 779*, 381–401.
Chapman, D., & Hayward, J. A. (1985) *Biochem. J. 228*, 281–295.
Chaudhuri, S. R., & Yang, J. T. (1968) *Biochemistry 7*, 1379–1383.
Dasseux, J.-L., Faucon, J.-F., Lafleur, M., Pézolet, M., & Dufourcq, J. (1984) *Biochim. Biophys. Acta 775*, 37–50.
Dluhy, R. A., Cameron, D. G., Mantsch, H. H., & Mendelsohn, R. (1983) *Biochemistry 22*, 6318–6325.
Gaber, B. P., & Peticolas, W. L. (1977) *Biochim. Biophys. Acta 465*, 260–274.
Gad, A. E. (1983) *Biochim. Biophys. Acta 728*, 377–382.
Gad, A. E., Silver, B. L., & Eytan, G. D. (1982) *Biochim. Biophys. Acta 690*, 124–132.
Galla, H.-J., & Sackmann, E. (1975a) *Biochim. Biophys. Acta 401*, 509–529.
Galla, H. J., & Sackmann, E. (1975b) *J. Am. Chem. Soc. 97*, 4114–4120.
Hammes, G. G., & Schullery, S. E. (1970) *Biochemistry 9*, 2555–2563.
Hartmann, W., & Galla, H. J. (1978) *Biochim. Biophys. Acta 509*, 474–490.
Hartmann, W., Galla, H. J., & Sackmann, E. (1977) *FEBS Lett. 78*, 169–172.
Kauppinen, J. K., Moffatt, D., Mantsch, H. H., & Cameron, D. G. (1981) *Appl. Spectrosc. 35*, 271–276.
Kimelberg, H. K., & Papahadjopoulos, D. (1971) *J. Biol. Chem. 246*, 1142–1148.
Levin, I. W., Mushayakarara, E., & Bittman, R. (1982) *J. Raman Spectrosc. 13*, 231–234.
Liao, M. J., & Prestegard, J. H. (1981) *Biochim. Biophys. Acta 645*, 149–156.
O'Leary, T. J., & Levin, I. W. (1984) *J. Phys. Chem. 88*, 4074–4078.
Ranck, J. L., & Tocanne, J.-F. (1982) *FEBS Lett. 143*, 175–178.
Savoie, R., Boulé, B., Genest, G., & Pézolet, M. (1979) *Can. J. Spectrosc. 24*, 112–117.
Shafer, P. T. (1974) *Biochim. Biophys. Acta 373*, 425–435.
Smith, R., Cornell, B. A., Keniry, M. A., & Separovic, F. (1983) *Biochim. Biophys. Acta 732*, 492–498.
Snyder, R. G., Hsu, S. L., & Krimm, S. (1978) *Spectrochim. Acta, Part A 34A*, 395–406.
Snyder, R. G., Scherer, J. R., & Gaber, B. P. (1980) *Biochim. Biophys. Acta 601*, 47–53.
Szoka, F., & Papahadjopoulos, D. (1978) *Proc. Natl. Acad. Sci. U.S.A. 75*, 4194–4198.
Theretz, A., Ranck, J.-L., & Tocanne, J.-F. (1983) *Biochim. Biophys. Acta 732*, 499–508.
Tu, A. T. (1982) in *Raman Spectroscopy in Biology: Principles and Applications*, pp 187–233, Wiley, New York.
Watts, A., Harlos, K., & Marsh, D. (1981) *Biochim. Biophys. Acta 645*, 91–96.
Weinstein, J. N., Klausner, R. D., Inneraty, T., Ralston, E., & Blumenthal, R. (1981) *Biochim. Biophys. Acta 647*, 270–284.
Wilschut, J. (1982) in *Méthodologie des Liposomes* (Leserman, L. D., & Bardet, J., Eds.) p 131, Séminaires technologiques de l' INSERM, Les Editions de l'INSERM, Paris.